Reconstruction of residential buildings from multi-aspect InSAR data

A. Thiele, E. Cadario, K. Schulz, U. Thoennessen, and U. Soergel, *Member, IEEE*

***Abstract*— The spatial resolution of state-of-the-art synthetic aperture radar (SAR) sensors enables the structure analysis of urban areas. The appearance of buildings in magnitude images in settlements is dominated by effects of the inherent oblique scene illumination, such as layover, radar shadow and salient lines of bright scattering caused by direct reflection or multipath signal propagation. For example, in urban residential districts often salient pairs of parallel lines of bright magnitude are caused by gable-roofed buildings. The first line (closer to sensor) is due to direct reflection of planar roof parts of small or even zero incidence angle. The second line can be related to signal caused by a dihedral corner reflector built between ground and building wall. In this paper an approach is presented aiming at reconstruction of gable-roofed buildings by knowledge based analysis considering the mentioned SAR-specific effects. The estimation of building height is carried out by the extracted geometric parameters from the amplitude image. The resulting geometric model ambiguity can be solved by comparing simulated and real interferometric phases at the building location.**

The reconstruction results are quantitatively assessed by using a high-resolution LIDAR surface model, cadastral data and a orthophoto.

***Index Terms*— multi-aspect, high-resolution, InSAR, gable-roofed building reconstruction**

I. Introduction

THE SAR sensor principle requires oblique and side looking illumination of a scene, giving rise to phenomena such as foreshortening, layover, occlusions, total reflection, and multi-bounce scattering [1]. Especially in urban environment, these effects are frequently observed due to vertical walls, tilted roof faces, and the preferred right-angled structures of buildings. 3D building recognition exploiting these effects has been studied for city cores with high buildings [2], rural areas [3], and industrial plants [4], [5], [6]. In [7] a combined classification and height map retrieval was investigated on high-resolution InSAR data. Many additional building features become visible in such data, especially in the layover area, due to the dominant backscattering of façade, roof, and other structures [8]. Such prominent signatures are certainly to aspect or viewing angle change variant, which has to be considered in building recognition approaches. Based on simulation results of a parallelepiped of Franceschetti et al. [9], wall-ground double scattering and the combination of different flight directions are considered to be useful features for this task. Building recognition based on multi-aspect high-resolution data were proposed in [4] and [10], utilizing a stereoscopic sequence with varying off-nadir angle and an orthogonal image configuration, respectively.

Up to now mainly prismatic object models were the base for these studies. Often observable SAR signatures in dense urban areas with residential character are parallel lines. Focusing on the analysis of those, demands an enhancement of the model to a gable-roofed building. Corresponding simulation results of such building type were presented in [11], where the sensor close amplitude maximum results from direct reflection of roof and the sensor far maximum from the wall-ground double scattering. The distinction of such backscattering can be realized by the investigation of polarimetric data [12] as well as InSAR data. The interferometric phase distribution in layover areas was analyzed in [13], [14] and especially for different building models in [15].

In this paper, the SAR signature of gable-roofed buildings is analyzed. Furthermore, the exploitation of these effects for the extraction of building features is investigated and the benefit utilizing information from multi-aspect data is emphasized. The results of the approach are evaluated in comparison with ground truth data, given as LIDAR DSM (Digital Surface Model), cadastral data and orthophoto.

II. InSAR Signature of Gable-Roofed Building

The building signature in optical images is characterized by the central projection properties and is shown in Fig. 1 (first column). In contrast, SAR has a side looking viewing geometry and the range distance to the sensor defines the appearance of a building in the SAR image. The signature of flat and gable-roofed buildings, respectively, is characterized by a layover area, corner reflector between ground and building wall, roof signal, and a radar shadow region. The first building signal (i.e. smallest distance to the sensor) is the so-

A. Thiele, E. Cadario, K. Schulz and U. Thoennessen are with the FGAN-FOM Research Institute for Optronics and Pattern Recognition, Gutleuthausstr. 1, D-76275 Ettlingen, Germany; (phone ++49 07243 992 333, fax: ++49 07243 992 299, e-mail: {thiele, cadario, schulz, thoe}@fom.fgan.de). U. Soergel is with the Institute of Photogrammetry and GeoInformation, Leibniz Universität Hannover, Nienburger Str. 1, D-30167 Hannover, Germany, (phone ++49 511 7622981, fax: ++49 511 762 2483, e-mail: soergel@ipi.uni-hannover.de).

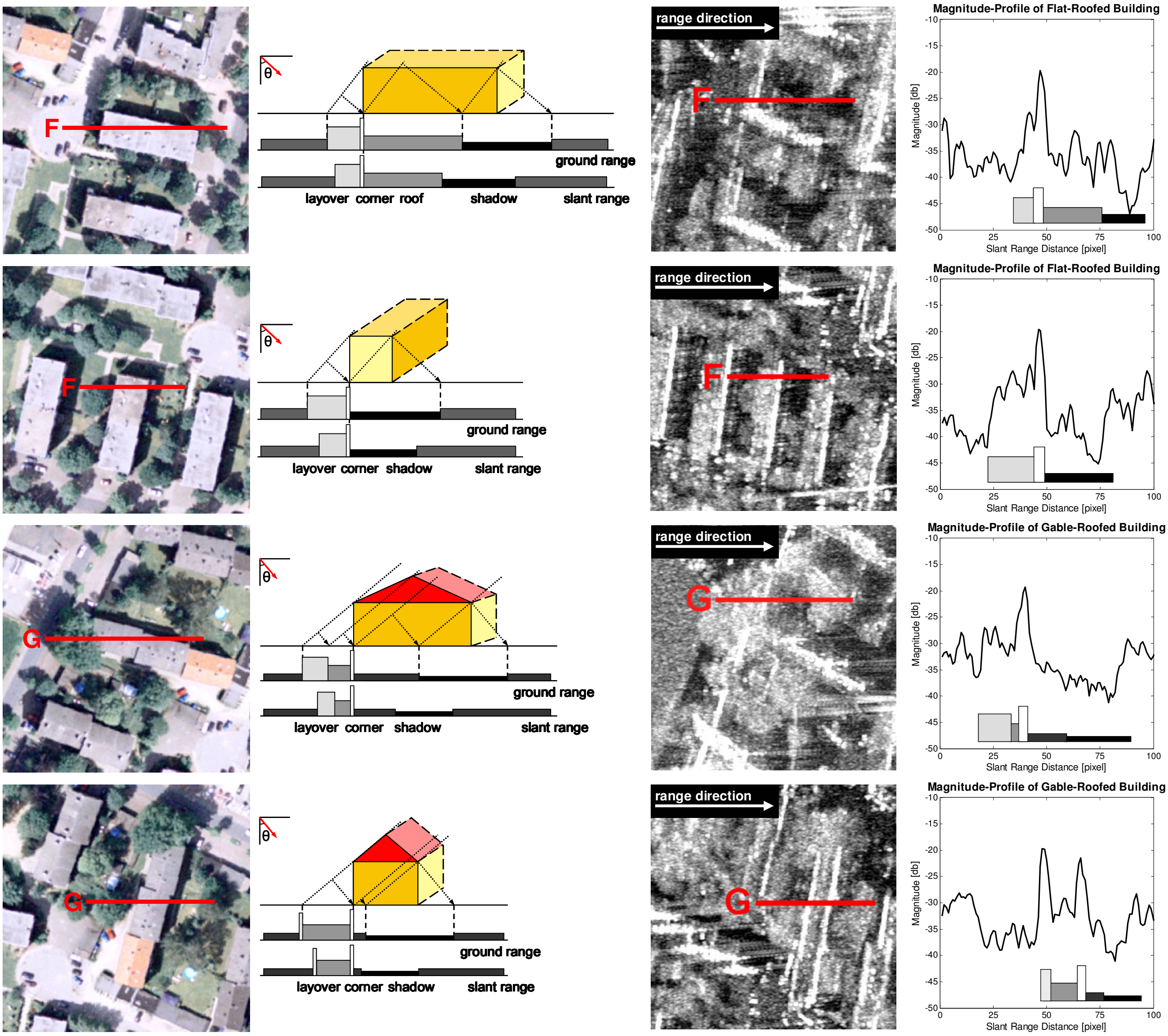

Fig. 1. Orthophotos of a residential scene (first column); illumination schemes and expected magnitude values in slant and ground range geometry (second column); real SAR signature of flat- and gable-roofed buildings in high-resolution multi-aspect data (third column); real SAR range profiles (marked in red – third column) at building location (fourth column); data of first aspect (first and third row), data of second aspect (second and fourth row).

called layover area, which appears usually bright due to a superposition of backscatter from ground, façade, and roof.

A schematic presentation of the expected SAR appearance of flat- and gable-roofed buildings under orthogonal illumination directions is depicted in Fig. 1 (second column). A corresponding scene is given in optical images (Fig. 1 first column) and SAR images (Fig. 1 third column).

Comparing the appearance of a flat-roofed building for the different illumination directions, a pure backscatter of the roof top is only observable if the building is long enough (Fig. 1 first row). Furthermore, a subdivision of the layover area is possible in some cases according to building dimensions and illumination geometry as described in [10], [16]. This effect occurs frequently at gable-roofed buildings, due to their pitched roof area (Fig. 1 third, fourth row).

The maximum amplitude and width of the first building signal (i.e. smallest distance to the sensor) depends on interrelation between roof pitch (α) and off-nadir angle (θ), as well as span angle. With increasing span angle between ridge orientation and azimuth direction the signature resemble more a flat-roofed building. This becomes clear considering the extreme case of ridge line parallel to range direction: there the roof height in a single range line is approximately constant. The brightest signal appears if the off-nadir angle equals the pitch angle (i.e. zero incidence angle, Fig. 1 fourth row). In Fig. 1 (third, fourth column) building signatures in real SAR data are given. Their magnitude distribution underlines the theoretically described backscatter phenomena.

The appearance of this significant signature of gable-roofed buildings (“double lines”) depends as well on the building geometry (e.g. height and roof-pitch α) as discussed in [17].

Investigating this described feature (“double lines”), two

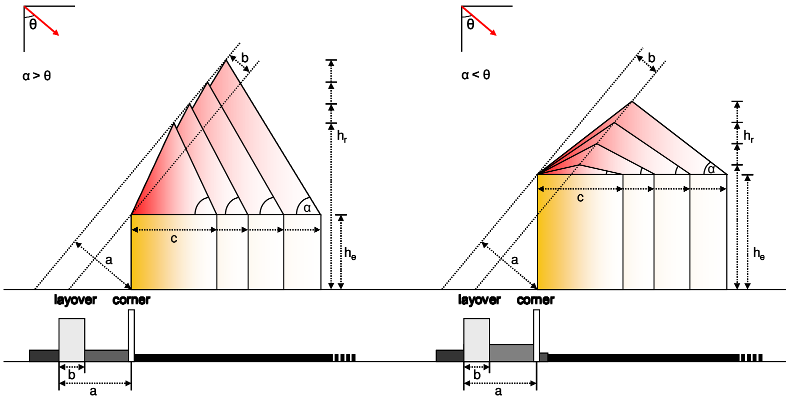

Fig. 2. Comparable magnitude distributions corresponding to different building models

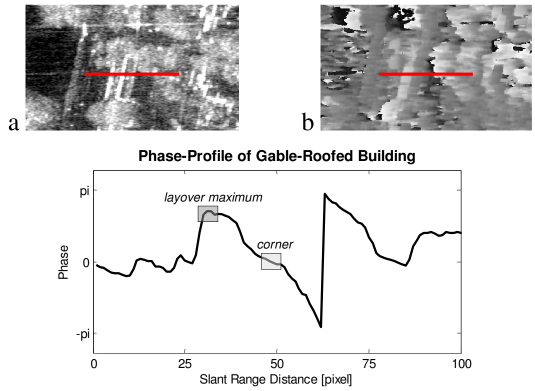

Fig. 3. SAR magnitude signature (a), InSAR phase signature (b) of a gable-roofed building; InSAR range phase profile (in (a) and (b) red marked)

building parameters can be derived as depicted in Fig. 2. These are distance between maxima (parameter a) and width of layover maximum (parameter b). Based on these parameters different building hypotheses can be formulated as illustrated in Fig. 2. The two groups of buildings are characterized by the different relations: $\alpha > \theta$ and $\alpha < \theta$. Assuming a multi-aspect data set, preferentially with orthogonal viewing direction, a restriction of these hypotheses is possible. From this second viewing direction the width of the building (parameter c), is extractable. Based on these three parameters, the ambiguity problem can be reduced to two building hypotheses. In the first case the roof pitch α is greater than the off-nadir angle θ, in the second one vice versa. In Fig. 2 h_e defines the height from ground up to eaves and h_r up to ridge. In (1) and (2) h_e, h_r, and α are given for the two cases.

$$\alpha > \theta, \qquad h_e = \frac{(a-b)}{\cos\theta} \qquad h_r = h_e + \frac{c}{2}\cdot\tan\alpha \qquad \tan\alpha = \tan\theta + 2\frac{b}{c\cdot\cos\theta} \tag{1}$$

$$\alpha < \theta, \qquad h_e = \frac{a}{\cos\theta} \qquad h_r = h_e + \frac{c}{2}\cdot\tan\alpha \qquad \tan\alpha = \tan\theta - 2\frac{b}{c\cdot\cos\theta} \tag{2}$$

The determination between the resulting two building hypotheses can carried out by investigation in the interferometric phases. Next to the significant magnitude signature of gable-roofed buildings, also their interferometric phases, especially in the layover area, show a distinctive distribution (Fig. 3). The calculated phase value of a single range cell results also from a backscatter mixture of different contributors (e.g. layover - ground, wall, and roof). In previous work [14] range profiles of the interferometric phase data in layover areas at buildings have been investigated. The shape of the phase profiles in theses so-called front-porch regions is to a large extent dominated by illumination direction and building geometry. The layover and corner line maxima in the magnitude image coincide with distinctive points in the phase profile (Fig. 3). Therefore, the phase data are used to discriminate both features robustly. Additionally, the ambiguity problem between the two building hypothesis can be solved by comparison of real interferometric phases and simulated phases at building location.

III. Real InSAR Data

The investigated single look complex InSAR data set was recorded by the AeS-1 sensor system of Intermap Technologies (X-Band) [18]. The spatial resolution is about 38 cm in range and 16 cm in azimuth direction, off-nadir angle variation is from 28° up to 52°, and the effective baseline 2.4 m. The test area was mapped in HH-polarization from two different aspects, spanning an angle of approximately 90°. The building inventory in this region is characterized by industrial areas and areas with groups of gable-roofed buildings. The latter are considered here. The pitch sides of the buildings were almost oriented in parallel to the sensor flight path.

IV. Algorithm

The presented approach aims at reconstruction of gable-roofed buildings from multi-aspect InSAR data. The underlying building model is characterized by a right-angled footprint and a symmetric gable roof.

A. *Segmentation of Primitives*

The segmentation of primitives exploits the discussed signature of gable-roofed buildings in the magnitude images. The line and edge detection is carried out by an adapted ratio edge detector according to [19].

The resulting segments are fitted to straight lines and edges, respectively, by linear approximation and subsequent prolongation.

B. *Extraction of Building Features*

In the first step the extraction of aforementioned parameters a, b is done in slant range geometry. The detected line and edge primitives are assembled to parallel line pair objects. The distance between the edge, detected on the sensor close side of

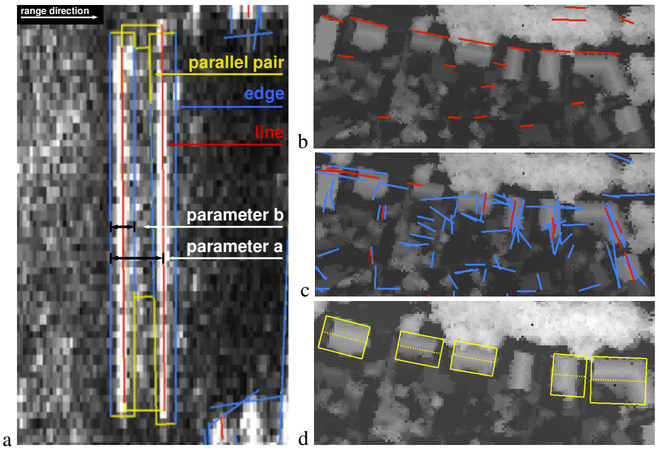

Fig. 4. Magnitude image overlaid with detected line, edges, parallel pairs and extracted parameters *a* and *b* (a); LIDAR DSM overlaid with orthorectified ridge-parallel corner lines (b, red), with ridge-perpendicular lines (c, red) and edges (c, blue) and reconstructed gable-roofed building footprints (d, dot-marked ridge)

the first maximum, and the line of the second maximum (corner line) define parameter *a*. The parameter b results from the distance between the enclosing edges of the first maximum (Fig. 4a).

Afterwards from the adjacent areas in the coinciding InSAR elevation data the mean height of each primitive is estimated [10]. The geocoding of the primitives is carried out with these estimated InSAR heights. The resulting geographic positions of the primitives are given in Fig. 4b,c.

In this common coordinate system the fusion of the primitives from the different aspects is feasible and hence the third parameter *c* (building width) can be extracted. Therefore, L-structures are assembled [8], by combining ridge-parallel corner lines resulting from first aspect and ridge-perpendicular lines or edges from second aspect, and vice versa. If there exists more than one L-structure per building, caused by more than one detected ridge-perpendicular line or edge for the same building, then a mean value is calculated for the building width *c*.

C. Generation of Building Hypotheses

The building generation is carried out in the common world coordinate system of the multi-aspects, and starts with the generation of the building footprint. Therefore, based on the position of a ridge-parallel corner line and the extracted corresponding width *c*, a rectangle object is assembled (Fig. 4d, Fig. 5). According to the mentioned model assumptions (right-angled footprint and symmetric gable roof) the position of the ridge is estimated. In order to derive a 3D model, the building height has to be inferred from the data. The calculation of the parameters h_e and h_r, according to (2) and (3), exploits the parameters *a*, *b* and *c*. Two 3D building models per footprint are possible. The ambiguity of these building hypotheses can probably be solved by analyzing the full interferometric phase distribution in the layover area, but this will be part of future work.

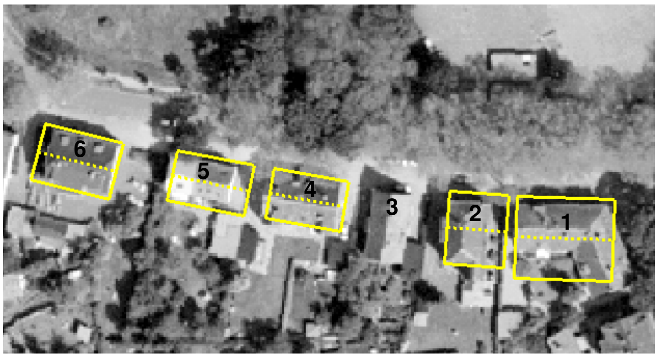

Fig. 5. Orthophoto (a) overlaid with reconstructed gable-roofed building footprints (dot-marked ridge)

D. Simulation of InSAR phases

Our process of interferometric phase simulation, presented in [15], takes into account that especially at building locations a mixture of several contributions can define the interferometric phase of a single range cell.

Based on the assembled building hypotheses and the extracted building heights, a ground range profile is defined. For this reconstruction task, two ground range models are extracted. Those and the resulting phase profiles are depicted in Fig. 6a,b.

In the case of parallel orientation of azimuth direction and detected corner line, only one ground range profile is necessary. This geometric constellation is fulfilled for the considered group of gable-roofed buildings. Consequently, the simulated phase range profile, orthogonal to the corner line (Fig. 6c) is constant.

E. Assessment of Building Hypothesis

One way to resolve the ambiguity problem of building hypotheses is the simulation of the interferometric phases in the layover area. The subsequent comparison with the real interferometric phases at the same location gives one model priority.

For assessment of the similarity between the simulated and real phase areas the correlation coefficient is used. An area of real interferometric phases is extracted along the detected corner line (Fig. 6d). Based on the restrictions of our simulation process, only the phase distribution in the layover area is considered in the calculation of the correlation coefficient.

V. Results

The approach was applied on a test site of six buildings (Fig. 5) of an average size of 18m x 10m x 12m (length x width x height). Four buildings (label 1, 4, 5, 6) show an almost parallel orientation between ridge and azimuth direction. Excluding building 1 and 2, which show an L-shaped footprint and a hip roof, respectively, fulfilled all other buildings the modeling assumptions (right angled footprint and gable roof).

The reconstructed width and length of the buildings as well

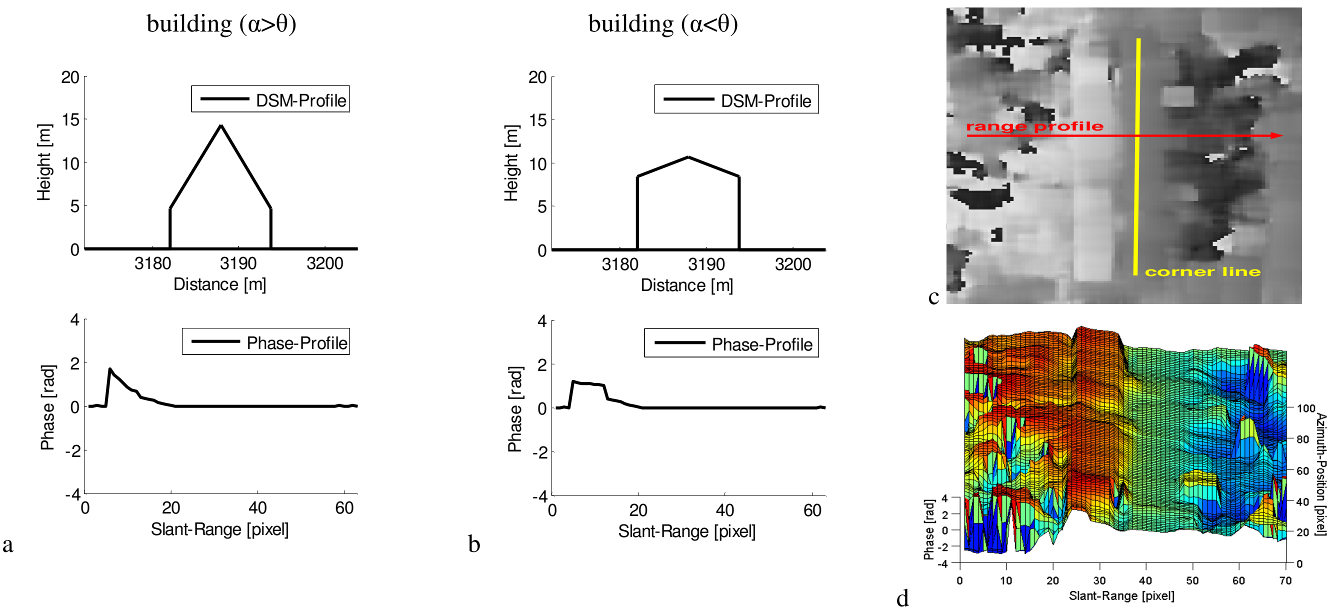

Fig. 6. Synthetic DSM profiles based on the two 3D building hypotheses and corresponding simulated phase profiles (a,b); real InSAR phases at building location overlaid with detected corner line (yellow) and range profile direction (red) (c); and real (d) phase distribution at building location.

TABLE I
3D RECONSTRUCTION RESULTS IN COMPARISON WITH GROUND TRUTH DATA

	Building Model		Building Model ($\alpha>\theta$)				Building Model ($\alpha<\theta$)				Ground Truth Data					
	length [m]	width [m]	h_e [m]	h_r [m]	α [°]	cc	h_e [m]	h_r [m]	α [°]	cc	length [m]	width [m]	h_e [m]	h_r [m]	α [°]	cc
1	22.7	19.1	5.3	18.6	54	0.60	9.0	14.9	31	0.61	20.0	10.0	7	12	45	0.53
2	13.7	17.0	7.5	19.7	55	0.30	11.2	16.0	29	0.35	10.0	14.0	9	12	23	0.41
4	17.6	11.8	4.7	14.3	58	0.72	8.4	10.6	20	0.74	16.8	11.1	7	11	39	0.66
5	18.0	*12*	4.6	14.3	58	0.00	8.3	10.6	21	0.07	14.1	8.0	6	10	45	0.39
6	18.6	13.5	4.2	14.6	57	0.22	8.0	11.0	24	0.26	15.4	12.0	7	12	40	0.34

as the cadastral data, are listed in Table I. Building 1 shows an oversized building footprint, but a correct detected ridge orientation. In comparison, building 2 shows the wrong ridge orientation but a well detected footprint. The reconstruction process delivered no result for building 3. The ridge orientation as well as the footprint of the buildings 4, 5 and 6 were well detected. Because of a lack of primitive objects for the second aspect, the width of building 5 is derived from building 4 and 6, assuming a row of buildings of similar type. Comparing the cadastral data with the reconstruction results, the lowest differences are given for building 4.

The 3D reconstruction results comprising building heights, corresponding roof pitch, and correlation results are summarized in Table I. In The second and the third column contain the reconstruction results of eave height h_e and ridge height h_r, as well as the correlation coefficient. The off-nadir angle θ is 45° for all buildings. In the last column the ground truth data extracted from the LIDAR DSM (Fig. 4d) are given. A rash preferring of one building model is not useful, because both constellations are covered in this urban area. Therefore, the correlation results have to be compared. There the higher correlation values are shown for model $\alpha < \theta$ (Table I), which is the final reconstruction result. The comparison with the ground truth heights shows differences from 0.4 m up to 4 m for this model. The assessment of the results for roof pitch α is less reliable, because the extraction of this ground truth value from a LIDAR DSM is inexact.

VI. CONCLUSION

The presented approach enables the reconstruction of gable-roofed buildings based on the signature in magnitude and interferometic phase images of a multi-aspect data set. The significant parallel line pairs are caused by the dominant backscattering of the roof in the layover area and the double bounce reflections between ground and façade (corner). Based on the width b of the layover maximum and the distance a between both lines building hypotheses are extractable. The investigation on multi-aspect data, enables additionally the extraction of the building width c, and consequently a reduction to two building hypotheses. Based on the real interferometric phases and the simulated phases, the assessment step delivers the final building model. The validation of the reconstruction results was done by using cadastral and LIDAR DSM data.

Future studies are focused on the investigation of non parallel configurations. The assessment of the building hypotheses based on the correlation coefficient has to be improved in the future. Furthermore, the accuracy and robustness of the parameter extraction *a*, *b* and *c* will be investigated and the integration of this approach in the existing work bench for building reconstruction will be done.

REFERENCES

[1] G. Schreier, “Geometrical Properties of SAR Images,” in *Schreier G. (ed) SAR Geocoding: Data and Systems*, Karlsruhe: Wichmann, 1993, pp. 103-134.

[2] P. Gamba, B. Houshmand, and M. Saccini, “Detection and Extraction of Buildings from Interferometric SAR Data,” *IEEE Transactions on Geoscience and Remote Sensing*, vol. 38, no.1, 2000, pp. 611-618.

[3] R. Bolter, “Buildings from SAR: Detection and Reconstruction of Buildings from Multiple View High Resolution Interferometric SAR Data,” Ph.D. dissertation, University Graz, 2001.

[4] E. Simonetto, H. Oriot, and R.Garello, “Rectangular building extraction from stereoscopic airborne radar images,” *IEEE Transactions on Geoscience and Remote Sensing*, vol. 43, no.10, 2005, pp. 2386-2395.

[5] U. Soergel, K. Schulz, and U. Thoennessen, “Phenomenology-based Segmentation of InSAR Data for Building Detection,” in *Radig, B., Florczyk, S. (eds) Pattern Recognition*, 23rd DAGM Symposium, Springer, 2001, pp. 345-352.

[6] F. Xu, and Y.-Q. Jin, “Automatic Reconstruction of Building Objects From Multiaspect Meter-Resolution SAR Images,” *IEEE Transactions on Geoscience and Remote Sensing*, vol. 45, no.7, 2007, pp. 2336-2353.

[7] C. Tison, F. Tupin, and H. Maître, “A Fusion Scheme for Joint Retrieval of Urban Height Map and Classification From High-Resolution Interferometric SAR Images,” *IEEE Transactions on Geoscience and Remote Sensing*, vol. 45, no. 2, 2007, pp. 496-505.

[8] U. Soergel, U. Thoenessen, A. Brenner, and U. Stilla, “High resolution SAR data: new opportunities and challenges for the analysis of urban areas”, *IEE Proceedings - Radar, Sonar, Navigation*, 2006.

[9] G. Franceschetti, A. Iodice, and D. Riccio, “A canonical problem in electromagnetic backscattering from buildings,” *IEEE Transactions on Geoscience and Remote Sensing*, vol. 40, 2002, pp. 1787-1801.

[10] A. Thiele, E. Cadario, K. Schulz, U. Thoennessen, and U. Soergel, “Building recognition from multi-aspect high resolution InSAR data in urban area,” *IEEE Transactions on Geoscience and Remote Sensing*, vol. 45, no. 11, 2007, pp. 3583-3593.

[11] F. Xu, and Y.-Q. Jin, “Imaging Simulation of Polarimetric SAR for a Comprehensive Terrain scene Using the Mapping and Projection Algorithm,” *IEEE Transactions on Geoscience and Remote Sensing*, vol. 44, no. 11, 2006, pp. 3219-3234.

[12] J.S. Lee, T.L. Ainsworth, E. Krogager, and W.M. Boerner, “Polarimetric Analysis of Radar Signature of a Manmade Structure”, in *Proceedings of IGARSS*, 2006, CD ROM, 4p.

[13] D.L. Bickel, W.H. Hensley, and D.A. Yocky, “The Effect of Scattering from Buildings on Interferometric SAR Measurements,” in *Proceedings of IGARSS*, Vol. 4, Singapore, 1997, pp. 1545-1547.

[14] A.J. Wilkinson, “Synthetic Aperture Radar Interferometry: A Model for the Joint Statistics in Layover Areas,” in *Proceedings of COMSIG*, Rondebosch, South Africa, 1998, pp. 333-338.

[15] A. Thiele, E. Cadario, K. Schulz, U. Thoennessen, and U. Soergel, “InSAR Phase Profiles at Building Locations,” *Proceeding of ISPRS Photogrammetric Image Analysis*, vol. XXXVI, part 3/W49A, pp. 203-208, 2007.

[16] G. Franceschetti, A. Iodice, D. Riccio, and G. Ruello, “SAR Raw Signal Simulation for Urban Structures,” *IEEE Transactions on Geoscience and Remote Sensing*, vol. 41, 2003, pp. 1986-1995.

[17] A. Thiele, E. Cadario, K. Schulz, U. Thoennessen, and U. Soergel, “Feature Extraction of Gable-Roofed Buildings from Multi-Aspect High-Resolution InSAR Data,” in *Proceedings of IGARSS*, 2007, CD ROM, 4p.

[18] M. Schwaebisch, and J. Moreira, “The high resolution airborne interferometric SAR AeS-1,” *Proceedings of the Fourth International Air-borne Remote Sensing Conference and Exhibition*, Ottawa, Canada, 1999, pp. 540-547.

[19] F. Tupin, H. Maitre, J-F. Mangin, J-M. Nicolas, and E. Pechersky, “Detection of Linear Features in SAR Images: Application to Road Network Extraction”, *IEEE Transactions on Geoscience and Remote Sensing*, vol. 36, no. 2, 1998, pp. 434-453.